Title:

Leishmania aethiopica cell-to-cell spreading involves caspase-3, AkT and NF-κB but not PKC-δ activation and involves uptake of LAMP-1 positive bodies containing parasites.

Medhavi Ranatunga[1#], Rajeev Rai[1,2#], Simon C. W. Richardson[1], Paul Dyer[1,3], Laurence Harbige[1,4], Andrew Deacon[1], Lauren Pecorino[1] and Giulia T. M. Getti[1*]

[1]*University of Greenwich at Medway, Central Avenue, Chatham Maritime, Kent ME4 4TB, UK*

[3]*Anglia Ruskin University, East Road, Cambridge CB1 1PT, UK*

*Corresponding author E-mail: G.T.M.Getti@gre.ac.uk, phone number: 02083318673

[#] contributed equally to the work

[2] current address*: University College London, GOS, 30 Guilford St, London WC1N 1EH*

[4] current address*: Faculty of Life Sciences and Computing, London Metropolitan University, 166-220 Holloway Road, London N7 8DB, UK*

Running title:

L. aethiopica **spreads between macrophages in LAMP-1 positive bodies after inducing host cell apoptosis.**

Keywords

apoptosis, *axenic amastigotes*, *L. aethiopica*, *L. mexicana,* infection spreading, GFP, THP-1, trafficking, EEA1 (Early Endosome Antigen 1), LAMP-1 (lysosomal-associated membrane protein 1).

Abbreviations

Akt: Protein Kinase B

BAD: BCL2 associated agonist of cell death

EEA 1: Early Endosome Antigen 1.

CF: PKC-δ cleaved fragment

CL: Cutaneous leishmaniasis

GFP: Green fluorescent protein

HI-FBS: heat inactivated foetal bovine serum

Ik-B: I kappa B

IF1: intermediate form 1

IL-1: interleukin 1

LAMP-1: Lysosomal-associated membrane protein 1

LPG: lipophosphoglycan

LPS: lipopolysaccharide

MCL: Mucocutaneous leishmaniasis

NF-kB: nuclear factor kappa-light-chain-enhancer of activated B cells

PBS: phosphate buffered saline

PMA: phorbol 12-myristate 13-acetate

PMN: polymorphonuclear neutrophils

PKC-δ: Protein kinase C delta

PS: phosphatidyl serine

RA: Retinoic acid

ROCK: Rho-associated kinase

SEM: scanning electron microscope

Ser: Serine

Thr: Threonine

TNF: Tumour necrosis factor

VL: Visceral leishmaniasis

7AAD: 7-aminoactinomycin D

Abstract

Development of human leishmaniasis is dependent on the ability of intracellular *Leishmania* parasites to spread and enter macrophages. The mechanism through which free promastigotes and amastigotes, bind and enter host macrophages has been previously investigated, however little is known about intracellular trafficking and cell-to-cell spreading. In this study, the mechanism involved in the spreading of *L. aethiopica* and *L. mexicana* was investigated. A significant increase in PS exhibition, cytochrome C release and active caspase 3 expression was detected ($P<0.05$) during *L. aethiopica*, but not *L. mexicana* spreading. A decrease ($p<0.05$) of Akt protein and BAD phosphorylation was also observed. The NF-kB signaling pathway and pro-apoptotic protein PKC-δ were downregulated while inhibition of caspase-3 activation prevented *L aethiopica* spreading. Overall suggesting that *L. aethiopica* induces host cell's apoptosis during spreading in a caspase-3-

dependent manner. The trafficking of amastigotes within macrophages following cell to cell spreading differed from that of axenic parasites and involved co-localization with Lysosomal-associated membrane protein 1 (LAMP-1) within 10 minutes post-infection. Interestingly, following infection with axenic amastigotes and promastigotes, co-localization of parasites with LAMP-1 positive structures took place at 1 and 4 h respectively, suggesting that the membrane coat and LAMP-1 protein was derived from the donor cell. Collectively, these findings indicate that host cell apoptosis, demonstrated by PS exhibition, caspase 3 activation, cytochrome C release, downregulation of Akt, BAD phosphorylation, NF-kB activation; and independent of PKC-δ expression, is involved in *L. aethiopica* spreading. Moreover, *L. aethiopica* parasites associate with LAMP-rich structures when taken up by neighbouring macrophages.

Introduction

Leishmaniasis is a widespread, neglected tropical disease for which no vaccine and limited treatment options exist. There are several barriers to the development of effective approaches for the prevention and treatment of leishmaniasis. These barriers include the ability of its causative agent, *Leishmania* to hide within host macrophages and successfully spread to neighbouring cells. Relatively little is known about intracellular trafficking of parasites within their long-term hosts, macrophages and consequent spreading. Of the over 20 species responsible for human infection only few have been investigated and intrinsic differences between species makes it difficult to generalise conclusions [1]. Recent findings suggest that *L. amazonensis*, *L. aethiopica* and *L. mexicana* but not *L. guyanensis* amastigotes induce host macrophages apoptosis [2–4]. Although apoptotic induction is thought to participate in the process of parasites egress within membrane bound bodies rich in late endosomal markers [4], very little is known about the biochemical pathways involved. At early stages of infection *Leishmania* are known to inhibit host cell apoptosis wih mechanisms involving a number of biochemical pathways. Following promastigote infection with *L. major*, *L. amazonensis* and *L. pifanoi*, the anti-apoptotic signalling PI3K/AKT is activated to confer resistance to the induction of macrophage apoptosis in murine models [5]. Interestingly, the survival of *L. donovani* in murine host macrophages was found to be linked to downregulation of NF-κB and the associated activation of the apoptotic pathway [6]. *L. infantum* infection was also able to reduce actinomycin D-induced apoptosis by impairing PKC δ cleavage in U-937 cells, suggesting a link between anti-apoptotic pathways and parasite survival in host macrophages [7]. The involvement of the above pathways with the process of amastigote spreading is not known and the molecular mechanisms behind apoptotic induction remain to be characterized. Interestingly very little is also known on what happens to parasites after they have been released from their

host cells, with only one study looking at the cell-to-cell spreading of intracellular parasites between human cells *in vitro* [2].

Promastigote and amastigote recognition, entrance and differentiation within macrophages have been studied in a number of *Leishmania* species and results have shown that species and stage-specific mechanisms are involved. *L. donovani* promastigote but not amastigote induce F-actin accumulation around the PV and the entrance of *L. infantum chagasi* promastigote (but not amastigote) was inhibited following lipid raft disruption [8,9]. It is less clear whether similar processes take place following the cell-to-cell spreading of amastigote. Until recently it has been widely accepted that free *Leishmania* amastigotes were released following host cell lysis and then subject to phagocytic capture by neighbouring macrophages. Later studies suggest that in some species a regulated mechanism of parasite release from macrophages can take place [4,10]. Very little information is available on whether this has an effect on entrance mechanisms and parasite trafficking inside the new host cells. Studies on cell-to-cell transfer of amastigote are limited, mostly because, until recently [2], an *in vitro* model of infection spreading between human cells has not been available.

In the present study, the mechanism behind intracellular amastigotes spreading and trafficking inside newly infected macrophages was investigated. Parasite spreading was associated with upregulation of apoptotic features (PS exhibition and Cytochrome C release) and linked to caspase 3 activation and downregulation of Akt, BAD phosphorylation, p65 and Ik-B and was independent of PKC-δ expression. Trafficking of *L. aethiopica* within host human macrophages was investigated by a co-localization approach using early and late endosome markers (*i.e.* EEA1 and LAMP-1). To detect differences between the uptake of free amastigotes and that of cell derived ones, *L. aethiopica* axenic amastigotes were developed. Different models of infection were then compared and model-dependent differences in parasites trafficking were reported. Co-localization between the parasite and EEA1 positive structures was investigated, with axenic amastigotes colocalising at 10 min and up to 4 h after infection. Colocalization with EEA-1 positive compartments often occurs within 5-10 min of entry via the endocytic system, prior to translocation to other sub-cellular organelles (e.g., late endosome, Golgi apparatus) within 1 h [11,12] The prolonged retention of axenic amastigotes within EEA-1 positive structures suggests a mechanism of interaction with the endosomal sorting machinery. Infection with promastigotes, on the other hand, failed to identify co-localization with EEA1 positive compartments, consistent with a previous report indicating an alternative pathway of entry for *L. infantum chagasi* promastigotes via cholesterol-rich domains, avoiding EEA-1 positive structures [8]. Furthermore, colocalization was observed with LAMP-1 positive (late endocytic) structures at four hours post-infection and retained for up to 24 hours. Of interest, was the finding that axenic amastigote

colocalization with LAMP-1 positive structures was observed at 1 hour post-infection suggesting an alternative mechanism of entry, possibly via a non-caveolae pathway. Analysis of spreading of amastigotes from infected cells indicated the existence of a third mechanism. Exposure to amastigotes derived from infected cells resulted in rapid co-localisation (less than 10 min) with LAMP-1 positive structures, consistent with the theory that parasites can enter the new host cell while still associated with LAMP-1 positive membrane from the donor cell. Supporting the notion that, similarly to *L. amazonensis*, intracellular *L. aethiopica* spreading between host cells does not necessitate release of extracellular parasites.

Results

Leishmania spreading correlated with host cell externalization of PS

Although a link between Leishmania infection and apoptosis has been clearly evidenced by several reports, whether and how induction of apoptosis is linked to infection spreading in human cells remains unexplored. The recent development of an in vitro model of infection spreading in human cells [2] allowed us to further investigate such possibility. One of the first changes that take place during apoptosis is the externalization of PS. PS is normally present on the macrophage membranes but is asymmetrically distributed on the cytosolic side by the action of ATP-dependent enzymes known as floppases [17]. Apoptotic cells on the other hand expose PS residues othe outer leaflet of the plasma membrane. Externalization of PS is a well-known induction signal for phagocytosis [18] which makes its presence during spreading of particular relevance.

Spreading of parasites between cells was induced in a donor population of cells by early camptothecin treatment as previously described [2]. Following 72 hours infection the donor population was co-cultured with a newly differentiated set of THP-1 cells (recipient population). Within this model spreading is known to take places within the first 24 hours from co-culture corresponding with the detection apoptotic markers. The percentage of cells expressing PS on the outer leaflet of their intact plasma membrane (PS+/7AAD-) at 1, 12 and 24 hours following co-culture is shown in Figure 1. Percentage of apoptotic cells was detected for the total cell population (Fig 1A) as well as the 2 sub-populations of infected (Fig 1B) and non-infected cells (Fig 1C) separately via flow cytometry as described in Material and Methods. The result showed a significant increase in the percentage of THP-1 cells expressing PS ($p<0.05$) co-cultured with enriched *L. aethiopica*^{GFP} infected cells compared with the control populations (Fig 1). The negative control population consisting of co-cultures with the uninfected THP-1 cells (RA treated and camptothecin treated) displayed no significant changes in apoptosis within 12 hours (Figure 1A). The results suggest the effect on apoptotic induction was not depndent on the characteristics of the uninfected donor cell populations but was associated with the

presence of the intracellular amastigotes. This is further confirmed by the fact that no significant differences in the percentage of 7AAD positive cells was detected in either time point following co-culture with infected or non-infected cells respectively (Figure 1C).

Leishmania spreading link with caspase-3 activation.

Apoptotic cell death can follow either caspase-3 dependent or independent pathways [19]. Activation of caspase 3 is associated with ROCK (Rho-associated kinase) activation and induction of cell blebbing. If apoptosis induction is the mechanism through which extrusion via formation of apoptotic bodies is initiated, it is expected that caspase 3 activation would significantly increase during spreading. To assess whether *Leishmania* utilizes a caspase-3 dependent pathway to initiate apoptosis, the expression of activated caspase-3 was detected at several time points after co-culture with cells infected with *L. aethiopica* and *L. mexicana.* Flow cytometry analysis showed a species-specific and time dependent response (Figure 2A, B). Following co-culture with *L. aethiopica* infected cells the percentage of cells expressing active caspase-3 at 1 hour was comparable to uninfected controls but significantly increased from 3 to 12 hours ($p<0.05$) post-infection. Interestingly, no significant differences were detected following co-culture with *L. mexicana* infected cells at any time point tested.

To test whether caspase-3 activation is critical for parasite dissemination, the infected co-culture was incubated in the presence of caspase-3 inhibitor, Z-DEVD-fmk. Z-DEVD-fmk is a tetrapeptide caspase inhibitor that is considered selective for caspase-3 and has been widely used in both *in vitro* and *in vivo* models to investigate roles for caspase 3 in cell death [20,21]. The results showed that pre-treatment with 100 μM but not 25 μM significantly ($p<0.05$) reduced the percentage of active caspase-3 at 3 and 12 hours respectively, when compared to non-treated infected co-cultures (Figure 2C). Interestingly, this inhibitory effect was associated with a significant reduction in the percentage of infected cells compared to non-treated sample at 12 hours (Figure 2D). Together the above findings demonstrate that amastigotes of *L. aethiopica,* but not *L. mexicana,* induce caspase-3 activation and that cell-to-cell spreading of *L. aethiopica* is impaired by caspase 3 inhibition.

De-regulation of AKT signaling pathway during *L. aethiopica* spreading

Activation of caspase-3 in apoptotic cells is regulated upstream by the AKT signalling pathway. In physiological states, phosphorylation of Threonine (Thr) 308 and Serine (Ser) 473 residues results in AKT activation, via phosphorylation, and attenuates the pro-apoptotic protein, BAD [22]. This effect inhibits the release of cytochrome C from mitochondria, hence preventing caspase-3 activation. If caspase 3 activation is

induced via AKT pathway a reduction in AKT phosphorylation of both Thr 308 (p-AKT Thr308) and Ser 473 (p-AKT Ser473) residues is expected. Expression of total AKT as well as (p-AKT Thr308) and p-AKT Ser473 was analyzed via western blot using β-actin as a loading control (Figure 3A-C and F). At 1 hour of co-culture, a significant decrease in band intensity was detected for both Thr 308 and Ser 473 residues of AKT in *L. aethiopica* infected cells compared to uninfected control (Figure 3A, B and F). Interestingly, from 6 hours onwards, there was approximately a twofold reduction of total AKT in the infected co-culture when compared to control, suggesting inhibition of AKT expression takes place following dephosphorylation of p-AKT (Figure 3C and F).

To confirm whether the decrease in AKT expression translated into downregulation of BAD activation, cell lysates from the infected co-cultures were assessed for the expression of BAD protein and phosphorylated BAD (Ser136) through western blot. The result showed a significant reduction in BAD phosphorylation compared to the control throughout all time points tested from 1 to 24 hours (Figure 3D and F). Overall BAD expression on the other hand remained constant throughout the time period (Figure 3F), suggesting that AKT reduction positively enhances BAD de-phosphorylation during *in vitro* spreading without affecting expression of BAD.

Furthermore, to assess whether BAD de-phosphorylation affects mitochondrial permeability, the presence of cytochrome C in the cytosolic extract from infected co-culture was detected by western blot. Starting from 6 hours post-infection, release of cytochrome C was markedly increased, approximately two-fold, when compared to the control (Figure 3E, F). Since elevated levels of active caspase-3 was detected between 6 and 12 hours post co-culture, the combined results suggest a positive correlation between activated BAD, cytochrome C release and caspase-3 activation during *L. aethiopica* spreading.

Attenuation of NF-kB signalling pathway during *L. aethiopica* infection spreading

NF-kB is a nuclear factor that regulates DNA transcription of several genes, including those that control cell survival. Activation of NF-kB is linked to the production of anti-apoptotic proteins. Release of NF-kB from its inhibitor and its consequent translocation to the nucleus results in upregulation of apoptotic inhibitors, including XIAP or cIAP-1 which block the initiator caspase 9 and the effector caspase 3. Various stimuli including LPS, TNF-α and IL-1 results in phosphorylation of Serine 32 and 36 residues (Ser 32/36), polyubiquitination and subsequent degradation of the inhibitory Iκ-Bα, releasing the NF-κB dimers, principally p65-p50. The expression of phosphorylated Iκ-Bα (Ser 32/36), IkB and p65 was investigated via western blot.

A significant ($p<0.01$) decrease in phosphorylation was detected within infected co-cultures between 1 and 24 hours post co-culture, when compared to uninfected control co-cultures (Figure 4A, D). This was correlated to a significantly lower expression of total Iκ-Bα protein (Figure 4B, D) suggesting that p65 is free from its inhibitor Iκ-Bα. However, when the infected cell lysates were probed with p65 antibody, a marked reduction of total p65 protein was detected throughout the time period (Figure 4C, D), indicating a disruption in span style="font-family:'Times New Roman'">the NF-κB signalling pathway. Interestingly, unlike other Leishmania species [23], *L aethiopica* did not cause cleavage of p65 in infected cells as shown by the absence of a 35 kDa fragment (fig 4E).

Decrease of PKC-δ during *L. aethiopica* infection spreading

Leishmania is known to alter the macrophage PKC signalling pathways, which results in the disruption of reactive oxygen species production. Although PKC subtypes are known to have either pro or anti-apoptotic function, only PKC-δ has been studied so far in the field of Leishmania infection and host cell death. Previous work has shown that early stage *L. infantum* infection prevents actinomycin D induced host apoptosis via PKC-δ inactivation [7]. This inactivation was due to the ability of LPG molecule to inhibit PKC-δ cleavage, which was further associated with reduced expression of activated caspase-3. Since we have previously demonstrated caspase-3 involvement in cell-to-cell infection [2], an investigation was carried out to assess whether there is a link between the activation of caspase-3 and PKC-δ inactivation during *L. aethiopica*^{GFP} infection spreading. After isolating cell lysates at 1, 6, 12 and 24 hours, the infected co-culture was analysed for PKC-δ expression through western blot. A band of approximately 78 kDa representative of total PKC-δ protein was detected in the uninfected control group from 1 to 24 hours (Figure 4D, E). However, throughout the time period, the PKC-δ intensity was significantly reduced ($p<0.01$) in the infected co-culture (Figure 4D). Interestingly, this effect was not due to accumulation of PKC-δ cleaved fragment (CF) as there was no protein band present at 45 kDa which is the expected size of CF (data not shown). This observation clearly shows that caspase-3 activation during infection spreading is not linked to PKC-δ activation but results in parasite dependent downregulation of PKC-δ during infection spreading.

Generation and validation of *L. aethiopica* axenic amastigotes

Two previously used media (JH30 and UM54) [24,25] were tested for their ability to support *L. aethiopica* amastigote growth *in vitro*. Parasites were cultured under the same conditions and at the same time in both media and samples were taken at regular intervals until complete transformation into amastigotes was reached. The concentration of parasites in each media significantly differed with JH30 clearly supporting a

faster rate of replication. From day 5 parasites started replicating in JH30 medium at a rate of one division every 6 hours, in UM54 parasites did not enter a log phase of growth, suggesting that UM54 media does not support *L. aethiopica* amastigote replication (Figure 5A).

Leishmania morphology showed major changes in both media (Figure 5B). After 2 days the parasites moved closer together in clumps and their body shapes changed to oval/rounded. The parasites in JH30 were actively dividing while the flagella had generally begun to disassemble, whilst in UM54 media the cytoplasm appeared vacuolated. On day 7, parasites growing in JH30 showed no flagella and a small rounded shape, closely resembling intracellular amastigotes (Figure 5C). Promastigote-shaped parasites, that werecompletely absent in JH30, were still present in UM54 with long flagella (Figure 5B, day 7). Rounded parasites in UM54 were heavily vacuolated confirming that UM54 as an unsuitable media to support differentiation and growth of axenic *L. aethiopica* amastigotes. The amastigote-like parasites obtained in JH30 were successfully sub-cultured in cell-free medium for over a year.

A closer view of the transformation process of promastigote in JH30 media was obtained by SEM (Figure 5D-G). The population observed was heterogeneous with different shaped parasites representing the various stages of the transformation process (Figure 5E). A high percentage of parasites during the first and second day of transformation maintained the promastigote elongated shape but also appeared wider with a long flagellum (intermediate form1: IF1). IF1 appeared shorter when compared to a normal promastigote (Figure 5D), with a length between 5 and 10 μm and an increased diameter (the largest part of the body measuring between 3 and 5 μm). Together with IF1 a new form was observed indicated as intermediate form 2 (IF2). The rounded/oval body measured 4 to 6 μm in diameter and appeared shorter (5 to 8 μm) and rounded. The flagella measured at least half the size and, in some cases, just 20% of the promastigotes flagella length. From day 0 to day 7, small rounded bodies with long flagella (LF) can be found. When observed under an inverted microscope the latter were immotile suggesting that they represent a population of dead parasites. Finally, dividing parasites were observed (Figure 5F). From day 5 onwards small, rounded aflagelleted parasites resembling amastigotes (Figure 5G) were present in higher percentage until they became the only shape present in the sample. Differences within a transforming population such as the number of parasites that lose promastigote features and start transforming into amastigotes were quantified.

Both stationary phase promastigotes and newly generated axenic amastigotes in JH30 media were used to infect terminally differentiated THP-1 cells. As expected [26], amastigotes showed a significantly higher infectivity ($P<0.05$) than the promastigotes with 49 (SEM ±5)% infected cells obtained following infection with axenic amastigotes compared to 28 (SEM ±2)% infected cells following infection with

stationary phase promastigotes. Axenic amastigotes grown in JH30 media were therefore considered as good model for amastigotes infection and used to study intracellular trafficking following exposure to THP-1 cells.

Development of a cell to cell infection model, RA-L8G-THP-1

In order to compare trafficking of the parasite following infection with axenic amastigotes or cell-derived amastigotes, we used a modified version of a model of cell to cell spreading our group previously developed [2]. Adherent (PMA-treated) THP-1 cells (recipient cells) were co-cultured with non-adherent (RA-treated), THP-1 cells heavily infected with *L. aethiopica*^{GFP} (RA-L8G-THP-1) which acted as donor cells in the spreading model. A population of RA-treated infected cells was used to control for donor cell adherence, and thus being assessed as a recipient population, and were found not to adhere to the plate.

The percentage of infection in non-adherent (donor) and adherent (recipient) cells was analysed by flow cytometry over a 5 days period Within 1 h of infection with RA-L8G-THP-1 cells the percentage of infected recipient cells increased from 0 to 28% ($P<0.0001$). This was accompanied by a drop in the percentage of infected donor cells (Figure 6A) suggesting the rapid cell-to-cell spreading of the parasite. The percentage infected recipient cells doubled between 1 and 24 h post infection, whilst that of infected donor cells showed no significant changes ($P>0.05$). Interestingly the total number of donor cells significantly decreased after 1 hour ($P<0.05$), reaching a baseline at 48 hours (Figure 6B), confirming their role as parasite donors. The percentage of infection, between 24 and 96 hours, significantly decreased in both populations (Figure 6A). Such decrease in recipient cells could be due to experimental limitations, specifically time-limited effect of PMA on the terminal differentiation of THP-1 cells leading to their detachment and replication. Taken together these findings clearly show that parasites spread from donor to recipient cells within the first 24 hours of contact and intracellular parasites remain inside host cells for up to 96 hours. This confirmed the suitability of this infection model for further analysis of cell derived amastigote trafficking especially within the first 24 hours.

Early endosomal trafficking: Parasite, EEA1 co-localization.

Trafficking of *L. aethiopica* in all three infection models (metacyclic promastigotes, axenic amastigotes and amastigotes from RA-L8G-THP-1) was visualized via immunofluorescence microscopy. The generation and maturation of *L aethiopica* phagosomes was examined via detection of early endosomal marker EEA1. Early endosomal co-localization was studied from 10 min to 24 h after infection. In all biological replicates, EEA1 co-localization was absent after infection with metacyclic promastigotes and cell-derived intracellular amastigotes but present in axenic amastigote infection (Figure 7Ai, arrows). Axenic amastigotes binding

with THP-1 cells was detected at 5 min after infection, EEA1 co-localization was visible from 30 min and continued until 4 h after infection (Figure 7Aii). As expected the parasites were 5µm in size (Figure 7Ai, anti-GFP arrow). During this time period 1 to 4 parasites were detected in each THP-1 cell. EEA1 co-localization was not detected after 24 h of infection with the axenic amastigote.

Late endosomal trafficking: Parasite, LAMP1 co-localization.

Further maturation of the PV by fusion with late endosomes/lysosomes organelles was determined through LAMP-1 detection. Samples infected with metacyclic promastigotes, intracellular amastigotes from RA-L8G-THP-1 cells, and axenic amastigotes at different infection time points were stained in parallel. During infection with metacyclic promastigotes, LAMP-1 positive bodies were first detected at 4 h post-infection and remained evident until 72 hours (Figure 7Bii, arrow), no evidence of LAMP-1 positive bodies were found at 5, 10, 30 min and 1 h post-infection. Parasite morphology was round with absent flagella (Figure 7Bi). Microscope analysis showed that *L. aethiopica* promastigote infection creates tightly bound individual PVs which express LAMP-1 markers.

Following infection with axenic amastigotes at 10:1 ratio, PMA treated THP-1 cells were stained for LAMP-1 markers at different time points (10 min, 30 min, 1 h, 2 h, 4 h & 24 h). LAMP-1 positive bodies were visible from 1 h post-infection (Figure 7Ci) and no evidence of LAMP-1 positive bodies were found at 10 min and 30 min (Figure 7Cii).

As there is no indication that during natural infection amastigotes are freely released from infected cells, we also used a model whereby heavily infected cells (RA-L8G-THP-1) were used as *Leishmania*-donor cells [2] and freshly differentiated THP-1 (PMA treated) as recipient cells. Adherent recipient cells were stained with late endosomal markers LAMP-1 and studied within 24 h post-infection at different time points (10 min, 30 min, 1 h, 2 h, 4 h & 24 h). Interestingly LAMP-1 positive parasites were detected in adherent cell population within 10 min of the post-infection period and throughout all time-points (Figure 7Dii). Parasites showed morphology typical of amastigotes, round shaped with a size of 3- 5µm (Figure 7Di, arrow).

Discussion

Leishmania parasite enters mammalian immune system (PMN, Dendritic Cell, monocytes, B cells) following the bite of an infected sand fly and, if successful in establishing itself in macrophages, it will cause a variety of clinical manifestations. Parasites residing within the dermis cause ulcerative skin lesions (cutaneous leishmaniasis, CL), can spread to mucous membranes causing disfiguring lesions (mucocutaneous leishmaniasis, MCL), or move to internal organs causing lethal diseases (visceral leishmaniasis, VL).

Although partially species-specific, the factors determining the different disease manifestations remain largely uncharacterised. The low number of parasites inoculated by sand-flies coupled with the time required for symptoms to develop underlines the fundamental role of cell-to-cell parasitic spread in the manifestation of the disease.

Release of *Leishmania* from infected cells has been largely assumed to occur either via host cell lysis and/or via an exocytic like process. Such a mechanism has been previously observed for *Shigella flexneri*, *Listeria monocytogenes* and Influenza virus. Although evidence of cytolysin (parasite-derived membrane pore forming enzyme), was previously identified for *L. amazonensis* [27], whether such virulent factors lead to host cell lysis and subsequent parasitic release remains to be confirmed. More recently, evidence of parasitic release following apoptosis induction in some *Leishmania* species has been reported [2,4] . As promastigotes, harboured by apoptotic neutrophils, are known to transfer successfully to macrophages to establish the next stage of infection [28] it is possible that phagocytosis of apoptotic macrophages harbouring amastigotes can also take place. This is supported by the fact that increase in parasite number after infection is not associated with inflammatory lesions, which would likely develop after macrophage rupture [29]. Our findings confirmed the involvement of apoptosis in *Leishmania* infection in a species-specific manner. Increased expression of Caspase-3 was detected during *L. aethiopica* but not *L. mexicana* amastigote spreading between human macrophages. Moreover, caspase inhibition significantly reduced the percentage of *L. aethiopica*-infected cells. Interestingly, two anti-apoptotic signalling pathways: AKT and NF-kB, but not PKC□ were also shown to be significantly downregulated during spreading.

Induction of apoptosis involves a very complex and sophisticated signalling pathway that is tightly regulated at multiple points. Current literature reports *Leishmania* promastigotes regulate host apoptotic induction via two major signalling pathways: AKT and NF-κB in order to prolong the survival of the host cell [5,6,30]. However, such studies are limited to early stages of promastigote infection and provide no information on the effect of amastigote on host cell apoptosis. This research showed for the first time how *L. aethiopica* amastigotes disrupts the pro-survival pathways of human macrophages in order to promote apoptosis in a time dependent manner. During parasite spreading (from 3 to 24 Hours after co-culture and 72 hours following promastigote infection of the donor cell population) a significant reduction in AKT was detected, which led to BAD activation and cytochrome C release from mitochondria. This decrease could be due to the action of parasite-mediated host proteasome activation as in *Legionella pneumophilla* in which ubiquitination and degradation of AKT through proteasome activity takes place [31]. Further analysis showed that p65 subunit, which is the main transactivation domain of NF-κB, responsible for mediating anti-apoptotic gene expression, was also significantly reduced throughout parasite spreading. NF-κB

downregulation has been previously reported in *L. mexicana* amastigotes where cysteine peptidase caused degradation of p65 in infected mouse macrophages [32]. Moreover *L. donovani*, *L. major*, *L. mexicana*, and *L. braziliensis* have been shown to cleave NF−κB p65 via gp63 proteases [23]. Similar effects were also observed in poliovirus infection whereby viral protease C degraded p65 in infected HeLa cells [33]. However, it is interesting to note that other human pathogens have evolved diverse strategies to counteract NF-κB mediated apoptosis. *Yersinia* secretes YopJ effector to suppress the phosphorylation and degradation of IκB inhibitor, which prevents the release and nuclear migration of p65 causing apoptotic induction of epithelial cells [34]. Whereas, type 3 secretion protein VP1686 of *Vibrio* interacted with p65 in order to block the DNA binding activity of NF-κB that resulted in apoptosis of RAW macrophage [35]. It is interesting to note that *Leishmania* has been previously shown to prevent caspase-3 activation in order to inhibit apoptotic induction during early stage of infection [5,30]. This reveals an elegant strategy employed by *Leishmania* in order to survive and maintain its virulent cycle in the mammalian host; inhibit host cell apoptosis to protect its progeny but ultimately exploit such death process in order to spread. Interestingly, the percentage of necrotic cells as measured by 7-AAD+ remained similar to non-infected cells. This suggests that infected cells dying through apoptosis are immediately phagocytized by neighbouring macrophages without losing membrane integrity. The increased externalization of phosphatidyl serine (PS) in infected cells, which is also a signal for phagocytosis [36] supports this hypothesis. This also matches our recent live imaging observation, which showed the exiting of *L. aethiopica* and *L. mexicana* can occur without rupturing the donor-infected cells [2]. The externalization of PS on the cell surface is the result of phospholipid scramblase activation. This activation is regulated either by caspase-3 or AIF protein (independent of caspase-3). We showed for the first time that activated caspase-3 is one of the instrumental factors in initiating *L. aethiopica* spread,/span> since inhibition in caspase-3 activity prevented the propagation of infection. Whether or not caspase-3 independent mechanism, i.e. AIF activation, is also critical for apoptotic induction in *L. aethiopica* or other species requires further investigation.

Infection with *L. aethiopica* is responsible for all forms of cutaneous leishmaniasis, despite its flexibility, very little is known about the biology and pathogenesis of *L. aethiopica* at the molecular level compared to other *Leishmania* species. Few *in vitro* studies have clarified only some of the parasites characteristics in terms of host cells infectivity [2,37], profile of chemokine expression [38] drug sensitivity [39] with no studies available on trafficking of *L. aethiopica* and its association with early and late endosomal markers inside host macrophages. Moreover, no study has ever looked at the differences in trafficking between the 3 stages of any *Leishmania* parasites infection: promastigote, extracellular amastigotes and human cell-derived amastigotes. The trafficking of various cargo through the endocytic system and their

temporal delineation through a variety of subcellular compartments (e.g. LAMP positive structure) has been critical to initial attempts to define the endocytic pathway [40]. This work used GFP expressing *L. aethiopica* to study trafficking pathways of both stages of *Leishmania* life cycle (promastigotes and amastigotes) as well as amastigotes derived from infected cells. Promastigote infection is representative of establishment of early infection, while late stages of infection and spreading were investigated via newly developed axenic amastigotes and a novel cell-mediated infection model

The focus of this research was to follow the endocytosis of *L. aethiopica* to clarify whether parasite trafficking inside host macrophages differs between parasitic stage, as well as mode of spreading (cell-mediated or directentry of amastigotes). Promastigote infection of PMA treated THP-1 cells over a 4-day period did not show a significant change in the percentage of infected cells as detected by flow cytometry. Therefore, PMA treated THP-1 cells were not considered a good 'donor' for parasitic spreading, but cells remained terminally differentiated and supported infection up to 96 h making it ideal to study the establishment of infection and *Leishmania* trafficking over this timeframe.

L. aethiopica axenic amastigotes were generated and validated. Axenic amastigotes are expected to be able to revert back to promastigotes on transfer to promastigote growth conditions in the same way that intracellular amastigotes can [14,15,25]. *L. aethiopica* axenic amastigotes grown in JH30 for up to 2 weeks were successfully reverted back to promastigotes for a total of 8 times. The reversion process was completed in 5 days and the promastigotes obtained were able to replicate and reach stationary phase. As expected axenic amastigote infectivity was significantly higher than promastigote stages. This suggests that the parasites were a good model for amastigotes and were used for further investigation.

The results of co-localisation analysis are summarised in Figure 8. Immunofluorescence microscopy showed that axenic amastigotes followed early endocytic pathways. They co-localized with EEA1 positive structures from 10 min post-infection and were detected for as long as 4 h. Consistent with previous data on *L. chagasi* and *L. amazonensis*, transient co-localization of EEA1 was not detected from 10 min following promastigotes infection [8,41]. In *L. infantum chagasi* the temporary association with EEA1 was associated with calveolae-dependent phagocytosis and necessitated an intact lipid raft. Amastigote entrance on the other hand did not require caveolin-1 and was not affected by disruption of lipid rafts [8]. It remains to be established whether a similar mechanism takes place during *L. aethiopica* infection. Late endosomal co-localization was detected following both promastigote and amastigote infection but at different time points (Figure 8). Axenic amastigotes co-localized with LAMP-1 positive structures from one hour post-infection while promastigotes co-localized at 4 h. As expected, delay of late endosomal co-localization of promastigotes was detected when comparing to amastigotes which is consistent with the knowledge that

promastigotes inhibit phagolysosome biogenesis to evade its microbicidal activity [42–45]. Previously reported data showed a shorter delay for both amastigotes and promastigotes of *L. amazonensis* and *L. major* [41] which co-localized with LAMP-1 at 30 min after infection. This difference suggests that *L. aethiopica* promastigotes need longer compared to other species to establish itself inside the early endosome before being able to survive inside late endocytic structures.

For the first time, cell-mediated entrance of amastigotes could be analysed and results revealed a significant difference when compared with entrance of both promastigotes and axenic amastigotes (Figure 8). Parasites from infected cells co-localized with LAMP-1 within 10 min post-infection and remained detectable for up to 24 hours. Moreover, unlike axenic amastigotes, and similarly to promastigotes no co-localization with EEA1 was detected at any time point. The lack of co-localization with EEA1 suggests that cell to cell transfer of amastigotes follows a mechanism more closely related to the one described following promastigote phagocytosis than the one associated with axenic amastigote entrance into host macrophages. Our data have shown that at the time of infection, amastigotes within the donor population co-localise with LAMP-1. Interestingly, intracellular amastigotes of *L. amazonensis* have also been shown to spread to uninfected macrophages within LAMP-1 rich vesicles [4]. Taken together these findings support the theory that, similarly to *L. amazonensis*, during infection spreading *L. aethiopica* parasites leave the cells as amastigotes within membrane bound vesicle containing LAMP-1 markers.

In conclusion, this study showed how *L. aethiopica* amastigotes manipulates the host signalling pathways in order to disseminate and promote survival of its infectious progeny in a new macrophage niche. We have also shown for the first time how *L. aethiopica* entrance and trafficking within host macrophages is affected by cell-mediated spreading. Our data show that the mechanism through which promastigotes and amastigotes establish themselves in late phagosomes is not only stage dependent but also varies depending on the modality of infection. Amastigote entrance following cell to cell spreading differs from axenic amastigote infection supporting previous observations that some *Leishmania* species can spread between host cells through membrane-bound bodies. The exact mechanism of entrance, whether the whole infected cell acts as a Trojan horse and the true involvement of caveolae-mediated phagocytosis remains to be established.

Materials and Methods

Cell lines

1. THP-1

Human THP-1 cells, acute monocytic leukemia cell line (ECACC: 88081201) were obtained from the European Collection of Cell Cultures (ECACC) and maintained at 37ºC and 5% (v/v) CO_2 in RPMI-1640 (Fisher Scientific) supplemented with 1x (v/v) penicillin-streptomycin-glutamine (Fisher Scientific) and 10% (v/v) HI-FCS (Fisher Scientific) at a concentration of $2.5x10^5$ cells/ml.

2. Promastigotes

GFP expressing *L. aethiopica*^{GFP} (L8G) and *L. mexicana*^{GFP} (M5G) were previously generated from strain MHOM/ET/72/L100 [13]. Promastigotes were cultured in Drosophila Schneider medium (Invitrogen, UK) supplemented with 23% heat-inactivated foetal bovine serum (HI-FBS) (Invitrogen, UK) and 1x Penstrep (Invitrogen, UK) and G418 (Sigma, UK) at an initial concentration of $5x10^5$ cells/ml.

3. *L. aethiopica* axenic amastigotes

Stationary phase *L. aethiopica* promastigotes were harvested, washed twice in PBS and re-suspended at a concentration of $1.5x10^6$ cells per ml in a modification of JH30 medium [14] without Penicillin and Methyl cellulose and in UM54 medium [15]. The promastigotes were incubated in tissue culture flasks (Nunc, UK) at 32°C and the transformation process monitored under inverted microscope. Samples were taken daily during the transformation and morphological changes characterised via light and electron microscopy. Once transformed into amastigotes, the parasites were subcultured in UM54 or JH30 medium at pH 5.

Light microscopy of axenic amastigotes

Parasites were washed in PBS and centrifuged into poly-lysine treated slides at 1000g for 8 min with a Cytospin 4 Cytocentrifuge (Thermo Shandon, UK). *Leishmania* were fixed by washing the slide with 70% methanol (Sigma, UK) and stained using Leishman's stain (BDH Laboratory Supplies, UK).

Electron microscopy of axenic amastigotes

Parasites were harvested and washed twice in PBS to eliminate any trace of the medium. The pellet was then fixed in 2.5% (w/v) glutaraldehyde for a minimum of 2 h in the dark. The sample were then transferred in poly-Lysine treated aluminium foil and allowed to adhere by centrifugation. Following 4 steps of dehydration in increasing percentage of alcohol (50%; 70%; 90%; 100% (w/v); 30 sec to 1 min each) the samples were critically point dried in a K850 Critical Point Drier (Emitech, UK) and transferred in stubs. The

stubs were then coated with Gold in the polaron E5000 Sputter Coater (Quorum Technologies, UK) and kept in dry atmosphere until examined in a Cambridge Stereoscan 360 scanning electron microscope.

Amastigotes/ promastigotes reversion

Amastigotes cultures which were able to replicate and survive in JH30 medium for at least 3 weeks were harvested, washed in PBS and re-suspended in DMEM (Invitrogen, UK) supplemented with 10% HI-FBS at a concentration of 10^6 cells/ml. Once amastigotes reverted into promastigotes, they were cultured until they reached stationary phase and were then transformed back into amastigotes as described in 2.1.3.

Infection

1. Infection of RA treated THP-1 cells.

For validation of axenic amastigotes morphology and infectivity, THP-1 cells were transformed into non-adherent macrophages by 3 days treatment with 1μM retinoic acid (RA, Sigma, UK). Following RA removal cells were infected with stationary phase promastigotes and axenic amastigotes of *L. aethiopica* at a ratio of 10:1 and stained after 48 h incubation at 37°C and 5% (v/v) CO_2. Non-adherent cells were centrifuged into clean slide by Cytocentrifugation (800 x g) and fixed. Coverslips with attached macrophages were washed with warm PBS and fixed in 70% methanol (v/v). Giemsa stain (BDH Laboratory Supplies, UK) was diluted 20 times in water buffered pH 6.8 and added to the slides or to the wells containing coverslips. After an hour the stain was washed out twice with pH 6.8 buffered solution, dried with a tissue paper and left overnight to further air dry. Finally, Histomount (Sigma-Aldrich) was added and infected macrophages counted under light microscope. Each data set came from the average of three experiments each of which was done in triplicate. A minimum of 100 macrophages was counted for each slide.

For use as donor cells RA treated THP-1 cells were infected with stationary phase promastigotes *L. aethiopica* at a ratio of 10:1. Percentage of infection was maximised as previously described [2]. Briefly, treatment with 3 μM of camptothecin (Sigma-Aldrich) was carried out at 0 hours after infection. Excess camptothecin was washed away 5 hours after infection, and infected cells re-suspended in complete RPMI medium and incubated at 37°C in a humidified 5% CO2 incubator for 72 hours. Percentage of infection was detected via flow cytometry (Accuri C6, BD) and cells were used as donor to infect freshly differentiated RA treated THP-1 [2] or PMA treated THP-1.

In order to eliminate any artefact due to camptothecin treatment in infected donor population, controls cells consisting of non-infected, RA-treated and Camptothecin treated THP-1 cells were used to infect newly

differentiated THP-1 cells. All measurements of expression of apoptotic feature were compared to this control.

2. Infection of PMA treated THP-1 cells.

Metacyclic promastigotes axenic amastigotes and RA-treated infected THP-1 cells were used to infect terminally differentiated THP-1 cells at a 1:10, 1:5 and 1:1 ratio respectively. Infection was established after THP-1 cells were transformed into adherent macrophages by 24 hours treatment with 320nM Phorbol 12-myristate 13-acetate (PMA, Sigma-Aldrich). Stationary phase, metacyclic promastigotes were isolated via peanut agglutination from transgenic GFP-expressing parasites of all four species as previously reported [2]. Unbound promastigote parasites were washed off gently after 24 h. Infection was carried out over a five days period and the percentage of infection was detected via flow cytometer after detaching THP-1 cells with EDTA. Successful infection was further characterised after immunostaining via immunofluorescent microscopy.

Secondary infection was carried out using RA-treated infected cells to infect healthy PMA-treated THP-1 cells. A donor population of terminally differentiated THP-1 containing a high proportion of infected cells was generated as previously described [2] and incubated with PMA treated THP-1 at a 1:1 ratio. At appropriate time periods (between 10 min and 96 h depending on experiment parameters) supernatant with non-adherent cells and EDTA treated adherent cells were analysed independently via flow cytometer. Adherent cells were visualized via immunofluorescence microscopy.

Detection of apoptosis

1. Annexin V / 7AAD assay

PE Annexin V apoptosis kit I (BD Biosciences) was used to determine the externalization of phosphatidylserine (PS) and membrane permeability of the cell. Annexin V protein binds to PS, which is externalized during early stages of apoptosis, whereas 7AAD intercalates with the cellular DNA if the membrane is damaged during late stage of apoptosis (necrosis). The kit was used according to manufacturer protocol. Briefly, co-culture were centrifuged at 500 g for 10 minutes and washed twice with ice-cold 1× PBS. After re-suspension in 1× binding buffer at a cell concentration of 1×10^6 per ml, 100 µl of cells were stained with 5 µl of PE Annexin V and 5 µl of 7AAD and incubated for 15 minutes in the dark at room temperature. Finally, 400 µl of 1× binding buffer was added to the stained cells and the percentage of Annexin V positive / 7AAD negative (early apoptosis) and Annexin V positive / 7AAD positive (late apoptosis or necrosis) cells were analysed through flow cytometry within 1 hour of staining.

2. Caspase-3 enzymatic assay

The PE Caspase-3 detection kit (BD Biosciences) was used to measure the activation level of caspase-3 enzyme of the cell. The kit was used according to the manufacturer protocol. Briefly, cocultures were centrifuged at 500 g for 10 minutes before washing twice with ice-cold 1× PBS. The cells were incubated at 0-4°C for 20 minutes with 1× Perm and Fix buffer at a cell concentration of 2×10^6 per ml. After incubation, the cells were washed twice with 1× washing buffer before staining with PE anti-caspase-3 antibody (20 µl per $1x10^6$ cells). Following 30 minutes incubation in dark, stained cells were washed with 500 µl of 1× washing buffer. After final re-suspension in 400 µl of 1× washing buffer, the percentage of caspase-3 positive cells were analysed through flow cytometry within 1 hour of staining.

3. Inhibition of caspase-3 activity

Donor RA-L8G-THP-1 cells were pre-treated with 25 µM and 100 µM of Z-DEVD-FMK (BD Biosciences, UK) for 4 hours and incubated at 37°C in a humidified CO2 (5%) incubator. After washing with 1× PBS, the infected cells were co-cultured with freshly prepared batch of differentiated THP-1 macrophages at 1:1 ratio (infected cell per uninfected cell ratio). The percentage of infection and caspase-3 activity were determined at 3 and 12 hours after co-culture. Untreated infected cells were taken as a positive control.

Flow cytometry

Donor and acceptor cells were differentiated based on adherence, the accuracy of this approach was confirmed by the fact that donor cells were unable to adhere to either wells or coverslips over 72 H (data not shown). Non adherent infected cells were resuspended in media and analysed with flow cytometry as previously described [13]. Adherent cells were washed with warm PBS and treated with EDTA for 15 min at 37°C. Following media inactivation of EDTA cells were resuspended and run through the flow cytometer (C6 flow cytometer, BD Accuri, UK).

Following an initial gating with Forward scatter (FSC) and Side scatter (SSC) parameters (Figure 1i), the THP-1 population was further gated using a histogram plot to separate GFP positive (infected cell) from GFP negative (uninfected cell) population (Figure 1iii). For apoptotic analysis the blue laser was used to excite different types of fluorochromes, specific to GFP (FL1), PE Annexin V and PE Caspase-3 (FL-2) and 7AAD (FL-3). To distinguish between apoptosis and necrosis, the cells stained with Annexin V and 7AAD were divided into live cells (Annexin V negative / 7AAD negative), apoptotic cells (Annexin V positive / 7AAD negative), necrotic cells (Annexin V positive / 7AAD positive) and dead cells (Annexin V negative /

7AAD positive) (Figure 1iv). Furthermore, within infected cultures, the percentage of apoptosis from total population was sub-divided into infected only (Figure 1vi) and uninfected only (Figure 1v) population.

Western blot

Western blotting was performed using the Mini-PROTEAN® Tetra Cell and electroblotting system (BioRad, Hercules, CA, USA) following the manufacturer's instructions. Acrylamide containing resolving gels, 10% (w/v) were used, transfer was conducted at 400 mA for 60 min. Western blots were carried out to analyse the involvement of proteins associated with apoptotic pathways during *L. aethiopica*^{GFP} infection spreading specifically. AKT was detected by: anti-phospho (Thr 308) AKT, anti-phospho (Ser 473) AKT, anti-total AKT antibodies (Santa Cruz, UK); PKC by anti-total PKC- δ (Santa Cruz, UK); NF-κB by anti-total p65, anti-phospho (Ser 32/36) IκBα, anti-total IκBα (Santa Cruz, UK); Cytochrome C by anti-Cytochrome C (Santa Cruz, UK); BAD by anti- phospho (Ser 136) BAD, Anti-total BAD (Santa Cruz, UK); and β actin housekeeper by Anti- β actin (Santa Cruz, UK). All antibodies were diluted into PBS containing 0.01% (v/v) TWEEN20 (Sigma, Dorset, UK) and 5% (w/v) non-fat dried milk (Marvel, Premier Foods plc, St. Albans, UK). Briefly, from each incubation time point, $1x10^6$ cells were harvested, washed and lysed in RIPA buffer (Abcam, UK), supplemented with 1x protease cocktail inhibitor (Fisher Scientific). Protein concentration was determined through BCA absorbance assay kit (Fisher Scientific) and 20 μg proteins separated on a 10% Tris glycine SDS gels (Fisher Scientific) for 50 minutes under a constant 185 volts. Blocking step was performed overnight at 4°C with 5% non-fat dry milk TBS tween or 5% BSA, TBS tween solution (BioRad). Antibody hybridizations were performed at room temperature under gentle agitation for 1 hour. Between the blocking steps and after antibody hybridization, three PBS/TWEEN20 (0.01% v/v) washes were performed. The final wash was conducted with PBS only. Detection was carried out using ECL reagent (Fisher Scientific, UK) and X ray film (Fisher Scientific, UK). Exposed X-ray film was developed, scanned and analysed using NIH ImageJ, before normalizing the expression level of the target gene to that of a housekeeper (β actin).

Immunofluorescence microscopic staining.

THP-1 cells were seeded at $5x10^4$ cells/cm^2 on a 6-well plate containing 12mm cover slips, treated with PMA as previously described and infected with axenic amastigotes, metacyclic *L. aethiopica*^{GFP} promastigotes or donor RA-L8G-THP-1 cells. Primary antibodies: mouse anti-EEA1(BD Biosciences) (1:200), mouse H4A3 anti-LAMP-1 (DSHB[a]) (1:10) were used to detect early and late endosome and anti-Texas-Red (Invitrogen) (1:200) secondary antibodies were used for visualization as previously described

[16]. At selected time points (10 min to 72 h), cells were washed three times with 1x PBS and fixed with 2% PFA for EEA1 (early endosomal marker) and methanol for LAMP-1 stain (late endosomal markers).

For immunostaining with EEA1, cells were fixed with freshly prepared 2% PFA (Fisher Scientific) in PBS for 20 min at room temperature. Cells were then permeabilized in 0.2% Triton x-100 (Fisher Scientific) plus 50nM glycine for 20 min and blocked in blocking buffer (5% FBS in PBS) for 1 h to complete fixation. For immunostaining using LAMP-1, cells were fixed in pre-chilled methanol for 5 min and blocked for 1 h. Fixed THP-1 cells were incubated with primary antibodies (EEA1 & LAMP-1) for 1 h at room temperature, washed and then incubated with secondary antibodies (Texas-Red) overnight at 4^{o}C. Methanol fixation for LAMP-1 antbody staining washed the GFP expression of the parasites. Therefore, an extra staining step was carried out with α-GFP antibodies. Then cover slips were washed three times with 1x PBS and mounted with vectashield H-1200 mounting medium with DAPI stain. Finally, slides were examined microscopically.

Microscopic analysis

PMA treated THP-1 images were acquired using the Nikon ECLIPSE Ti-U inverted microscope attached to a computer running Nikon NIS-Elements Advanced Research software or an LSM880 Airyscan confocal microscope (Carl Zeiss Ltd, Germany). Immune stained fixed cells' images were acquired with the LSM880 using a 63x objective (Plan-Apochromat 63x/1.40 Oil DIC objective). Electron microscopy images were obtained through Cambridge Stereoscan 360 scanning electron microscope.

Quantification of co-localization

Co-localisation of amastigotes with either EEA1 or LAMP1 stained vesicles was performed using Image J. Individual images (green or red) were converted to 16-bit images, thresholds applied, and selected pixels overlaid and analysed for the proportion of co-localised (green with red) pixels. Percentage co-localisation was calculated as the proportion of green (amastigote) pixel count with the total red (TexasRed®) pixel count. Resultant percentages were plotted as vertical scatter plots with mean and standard error of the mean for each data point using GraphPad Prism v5.0.

Statistical Analysis

Data shown are representative of at least three independent experiments performed in three technical replicates. Data represents mean values with statistical error mean (SEM). Statistical analysis was performed using either ANOVA or student t test provided by GraphPad Prism (CA, USA) software and p values less than 0.05 ($P<0.05$) were considered significant differences between two independent samples.

References

1 Cohen-Freue G, Holzer TR, Forney JD & McMaster WR (2007) Global gene expression in Leishmania. *Int. J. Parasitol.* **37**, 1077–1086.

2 Rai R, Dyer P, Richardson S, Harbige L & Getti G (2017) Apoptotic induction causes Leishmania aethiopica and L. mexicana spreading in terminally differentiated THP-1 cells. *Parasitology*, 1–10.

3 DaMata JP, Mendes BP, Maciel-Lima K, Menezes CAS, Dutra WO, Sousa LP & Horta MF (2015) Distinct Macrophage Fates after in vitro Infection with Different Species of Leishmania: Induction of Apoptosis by Leishmania (Leishmania) amazonensis, but Not by Leishmania (Viannia) guyanensis. *PLoS One* **10**, e0141196.

4 Real F, Florentino PTV, Reis LC, Ramos-Sanchez EM, Veras PST, Goto H & Mortara RA (2014) Cell-to-cell transfer of Leishmania amazonensis amastigotes is mediated by immunomodulatory LAMP-rich parasitophorous extrusions. *Cell. Microbiol.* **16**, 1549–1564.

5 Ruhland A, Leal N & Kima PE (2007) Leishmania promastigotes activate PI3K/Akt signalling to confer host cell resistance to apoptosis. *Cell. Microbiol.* **9**, 84–96.

6 Singh KV, Balaraman S, Tewary P & Madhubala R (2004) Leishmania donovani activates nuclear transcription factor-κB in macrophages through reactive oxygen intermediates. *Biochem. Biophys. Res. Commun.* **322**, 1086–1095.

7 Lisi S, Sisto M, Acquafredda A, Spinelli R, Schiavone M, Mitolo V, Brandonisio O & Panaro M (2005) Infection with Leishmania infantum inhibits actinomycin D-induced apoptosis of human monocytic cell line U-937. *J. Eukaryot. Microbiol.* **52**, 211–217.

8 Rodríguez N, Dixit U, Allen L-A & Wilson ME (2011) Stage-specific pathways of Leishmania infantum chagasi entry and phagosome maturation in macrophages. *PLoS One* **6**, e19000.

9 Lang T, Hellio R, Kaye PM & Antoine JC (1994) Leishmania donovani-infected macrophages: characterization of the parasitophorous vacuole and potential role of this organelle in antigen presentation. *J. Cell Sci.* **107 (Pt 8**, 2137–2150.

10 Getti GT, Cheke RA & Humber DP (2008) Induction of apoptosis in host cells: a survival mechanism for Leishmania parasites? *Parasitology* **135**, 1391–9.

11 Dyer PD & Richardson SC (2011) Delivery of biologics to select organelles – the role of biologically active polymers. *Expert Opin. Drug Deliv.* **8**, 403–407.

12 Dyer PDR, Kotha AK, Pettit MW & Richardson SCW (2013) Imaging select mammalian organelles using fluorescent microscopy: Application to drug delivery. *Methods Mol. Biol.* **991**, 195–209.

13 Patel AP, Deacon A & Getti G (2014) Development and validation of four Leishmania species constitutively expressing GFP protein. A model for drug discovery and disease pathogenesis studies. *Parasitology* **141**, 501–510.

14 Pan A, Duboise SM, Eperon S, Rivas L, Hodgkinson V, Traubcseko Y & McMahon Pratt D (1993) Developmental Life Cycle of Leishmania: Cultivation and Characterization of Cultured Extracellular Amastigotes. *J. Eukaryot. Microbiol.* **40**, 213–223.

15 Balanco JM, Pral EM, da Silva S, Bijovsky AT, Mortara RA & Alfieri SC (1998) Axenic cultivation and partial characterization of Leishmania braziliensis amastigote-like stages. *Parasitology* **116 (Pt 2**, 103–113.

16 Richardson SCW, Wallom K-L, Ferguson E, Deacon SPE, Davies MW, Powell AJ, Piper RC & Duncan R (2008) The use of fluorescence microscopy to define polymer localisation to the late endocytic compartments in cells that are targets for drug delivery. *J. Control. Release* **127**, 1–11.

17 Daleke DL (2003) Regulation of transbilayer plasma membrane phospholipid asymmetry. *J. Lipid Res.* **44**, 233–242.

18 Grimsley C & Ravichandran KS (2003) Cues for apoptotic cell engulfment: Eat-me, don’t eat-me and come-get-me signals. *Trends Cell Biol.* **13**, 648–656.

19 Kulda K, Zheng TS, Na S, Kuan CY, Yang D, Karasuyama H, Rakic P & Flavell RA (1996) Decreased apoptosis in the brain and premature lethality in CPP32- deficient mice. *Nature* **384**, 368–372.

20 Garcia-Calvo M, Peterson EP, Leiting B, Ruel R, Nicholson DW & Thornberry NA (1998) Inhibition of human caspases by peptide-based and macromolecular inhibitors. *J. Biol. Chem.* **273**, 32608–32613.

21 Thornberry NA, Rano TA, Peterson EP, Rasper DM, Timkey T, Garcia-Calvo M, Houtzager VM, Nordstrom PA, Roy S, Vaillancourt JP, Chapman KT & Nicholson DW (1997) A combinatorial approach defines specificities of members of the caspase family and granzyme B: Functional relationships established for key mediators of apoptosis. *J. Biol. Chem.* **272**, 17907–17911.

22 Garcia-Echeverria C & Sellers WR (2008) Drug discovery approaches targeting the PI3K/Akt pathway in cancer. *Oncogene* **27**, 5511–5526.

23 Gregory DJ, Godbout M, Contreras I, Forget G & Olivier M (2008) A novel form of NF-κB is induced by Leishmania infection: Involvement in macrophage gene expression. *Eur. J. Immunol.* **38**, 1071–1081.

24 Pan A (1984) Leishmania mexicana: Serial cultivation of intracellular stages in a cell-free medium. *Exp. Parasitol.* **58**, 72–80.

25 Hodgkinson VH, Soong L, Duboise SM & McMahon-Pratt D (1996) Leishmania amazonensis: cultivation and characterization of axenic amastigote-like organisms. *Exp. Parasitol.* **83**, 94–105.

26 Gupta N, Goyal N & Rastogi AK (2001) In vitro cultivation and characterization of axenic amastigotes of Leishmania. In *Trends in Parasitology* pp. 150–153.

27 Noronha FSM, Cruz JS, Beirão PSL & Horta MF (2000) Macrophage damage by Leishmania amazonensis cytolysin: Evidence of pore formation on cell membrane. *Infect. Immun.* **68**, 4578–4584.

28 van Zandbergen G, Klinger M, Mueller A, Dannenberg S, Gebert A, Solbach W & Laskay T (2004) Cutting Edge: Neutrophil Granulocyte Serves as a Vector for Leishmania Entry into Macrophages. *J. Immunol.* **173**, 6521–6525.

29 Belkaid Y, Mendez S, Lira R, Kadambi N, Milon G & Sacks D (2000) A natural model of Leishmania major infection reveals a prolonged “silent” phase of parasite amplification in the skin before the onset of lesion formation and immunity. *J. Immunol.* **165**, 969–977.

30 Akarid K, Arnoult D, Micic-Polianski J, Sif J, Estaquier J & Ameisen JC (2004) Leishmania major-mediated prevention of programmed cell death induction in infected macrophages is associated with the repression of mitochondrial release of cytochrome c. *J. Leukoc. Biol.* **76**, 95–103.

31 Ivanov SS & Roy CR (2013) Pathogen signatures activate a ubiquitination pathway that modulates the function of the metabolic checkpoint kinase mTOR. *Nat. Immunol.* **14**, 1219–1228.

32 Cameron P, McGachy A, Anderson M, Paul A, Coombs GH, Mottram JC, Alexander J & Plevin R (2004) Inhibition of lipopolysaccharide-induced macrophage IL-12 production by Leishmania mexicana amastigotes: the role of cysteine peptidases and the NF-kB signaling pathway. *J Immunol* **173**, 3297–3304.

33 Neznanov N, Chumakov KM, Neznanova L, Almasan A, Banerjee AK & Gudkov A V. (2005) Proteolytic cleavage of the p65-RelA subunit of NF-κB during poliovirus infection. *J. Biol. Chem.* **280**, 24153–24158.

34 Schesser K, Spiik AK, Dukuzumuremyi JM, Neurath MF, Pettersson S & Wolf-Watz H (1998) The yopJ locus is required for Yersinia-mediated inhibition of NF-κB activation and cytokine expression: YopJ contains a eukaryotic SH2-like domain that is essential for its repressive activity. *Mol. Microbiol.* **28**, 1067–1079.

35 Bhattacharjee RN, Park KS, Kumagai Y, Okada K, Yamamoto M, Uematsu S, Matsui K, Kumar H, Kawai T, Iida T, Honda T, Takeuchi O & Akira S (2006) VP1686, a Vibrio type III secretion protein, induces Toll-like receptor-independent apoptosis in macrophage through NF-KB inhibition. *J. Biol. Chem.* **281**, 36897–36904.

36 Erwig LP & Henson PM (2008) Clearance of apoptotic cells by phagocytes. *Cell Death Differ.* **15**, 243–250.

37 Ogunkolade BW, Colomb-Valet I, Monjour L, Rhodes-Feuillette A, Abita JP & Frommel D (1990) Interactions between the human monocytic leukaemia THP-1 cell line and Old and New World species of Leishmania. *Acta Trop* **47**, 171–176.

38 Akuffo HO (1992) Cytokine responses to parasite antigens: in vitro cytokine production to promastigotes of L. aethiopica by cells from non-Leishmania exposed donors may influence disease establishment. *Scand. J. Immunol.* **11**, 161–166.

39 Utaile M, Kassahun A, Abebe T & Hailu A (2013) Susceptibility of clinical isolates of Leishmania aethiopica to miltefosine, paromomycin, amphotericin B and sodium stibogluconate using amastigote-macrophage in vitro model. *Exp. Parasitol.* **134**, 68–75.

40 Mullock BM, Smith CW, Ihrke G, Bright NA, Lindsay M, Parkinson EJ, Brooks DA, Parton RG, James DE, Luzio JP & Piper RC (2000) Syntaxin 7 is localized to late endosome compartments, associates with Vamp 8, and Is required for late endosome-lysosome fusion. *Mol. Biol. Cell* **11**, 3137–53.

41 Courret N, Fréhel C, Gouhier N, Pouchelet M, Prina E, Roux P & Antoine J-C (2002) Biogenesis of Leishmania-harbouring parasitophorous vacuoles following phagocytosis of the metacyclic promastigote or amastigote stages of the parasites. *J. Cell Sci.* **115**, 2303–16.

42 Dermine J-F, Scianimanico S, Privé C, Descoteaux A, Desjardins M, Prive C, Descoteaux A & Desjardins M (2000) Leishmania promastigotes require lipophosphoglycan to actively modulate the fusion properties of phagosomes at an early step of phagocytosis. *Cell. Microbiol.* **2**, 115–126.

43 Desjardins M & Descoteaux A (1997) Inhibition of Phagolysosomal Biogenesis by the Leishmania Lipophosphoglycan. *J. Exp. Med* **00**, 2061–2068.

44 Späth GF, Garraway LA, Turco SJ & Beverley SM (2003) The role(s) of lipophosphoglycan (LPG) in the establishment of Leishmania major infections in mammalian hosts. *Proc. Natl. Acad. Sci. U. S. A.* **100**, 9536–9541.

45 Scianimanico S, Desrosiers M, Dermine JF, Méresse S, Descoteaux A & Desjardins M (1999) Impaired recruitment of the small GTPase rab7 correlates with the inhibition of phagosome maturation by Leishmania donovani promastigotes. *Cell. Microbiol.* **1**, 19–32.

Legends

Figure 1.

Effect of *L. aethiopica*^{GFP} and *L. mexicana*^{GFP} infection spreading on host cell apoptosis. After infection of differentiated THP-1 macrophages with *L. aethiopica*^{GFP} and *L. mexicana*^{GFP} infected cells, the co-culture was analyzed for the percentage of apoptotic cells (Annexin V+/7AAD-) through flow cytometry at 1, 12 and

24 hours after co-culture. Apoptosis from the total population **(A)** were divided into infected only **(B)** and uninfected only **(C)** populations. **(i-vi)** Flow cytometry analysis of PE-Annexin V / 7-AAD stained cells. **(i)** The total population of differentiated THP-1 macrophages (double stained with PE-Annexin V and 7AAD) were initially gated as P4, according to FSC-A and SSC-A parameters. **(ii)** The doublet cells were excluded. Following exclusion, two plots were created. **(iv)** A dot plot comprising of PE-Annexin V (X-axis) versus 7-AAD (Y-axis) was created to isolate live (Q9-LL), early apoptotic (Q9-LR), late apoptotic (Q9- UR) and dead (Q9-UL) cells. **(iii)** A histogram plot comprising of GFP (X-axis) versus Count (Y-axis) was created to detect the percentage of infected cells in V1-R region from uninfected cells in V1-L region. **(v)** A dot plot comprising of PE Annexin V (X-axis) versus 7AAD (Y-axis) was created from V1-L region. This apoptotic plot corresponds to uninfected only population. **(vi)** Similarly, a dot plot comprising of PE Annexin V (X-axis) versus 7AAD (Y-axis) was created from V1-R region. This apoptotic plot corresponds to the infected only population. Uninfected cells co-cultured with differentiated THP-1 macrophages were taken as a positive control. The data represents mean percentage (mean ± SEM) from three independent experiments. Differences between infected cells co-culture and control were analysed through student *t* test. * = $p<0.05$. Flow cytometry images are an example from one representative experiment.

Figure 2.

Link between *L. aethiopica*^{GFP} and *L. mexicana*^{GFP} infection spreading and caspase-3 activation in host cells. **A-B**. Effect of *L. mexicana*^{GFP} infection spreading on the activation of caspase-3 in host cells. After re-infection of differentiated THP-1 macrophages with *L. aethiopica*^{GFP} (A) and *L. mexicana*^{GFP} (B) infected cells, the co-culture was analyzed for the percentage of activated caspase-3 through flow cytometry at 1,3, 6 and 12 hours after co-culture. Uninfected cells co-cultured with differentiated THP-1 macrophages were taken as a positive control. The data represents mean percentage (mean ± SEM) from three independent experiments**. C-D**: Effect of caspase-3 inhibition on the apoptosis and infection spread after infection with *L. aethiopica*^{GFP} infected cells. After *L. aethiopica*^{GFP} infected cell treatment with and/or without Z-DEVD-FMK for 4 hours, it was co-cultured with differentiated THP-1 macrophages. The co-culture was analyzed for the percentage of activated caspase-3 (**C**) and infection (**D**) through flow cytometry at 3 and 12 after co-culture. The data represents mean percentage (mean ± SEM) from three independent experiments. Differences between samples and control were analysed through student *t* test. * = $p<0.05$

Figure 3.

Effect of *L. aethiopica*^{GFP} infected cells on AKT, BAD and Cytochrome C during infection spreading. Following infection of differentiated THP-1 macrophages with *L. aethiopica*^{GFP} infected cells, whole cell lysates were collected at 1, 6, 12 and 24 hours after co-culture. Equal amounts of proteins were resolved by SDS-PAGE and analysed through western blotting. **A.** Densitometry analysis of p-AKT (Thr 308) expression. **B.** densitometry analysis of p-AKT (Ser 473). **C.** Densitometry analysis of total AKT. **D.** Densitometry analysis of p-BAD (Ser 136) expression. **E.** Densitometry analysis of Cytochrome C expression. **F.** Representative blots, left to right lane: 1h co-culture between uninfected donor and uninfected recipient → 1h co-culture between infected donor and uninfected recipient → 6h co-culture between uninfected donor and uninfected recipient → 6h co-culture between infected donor and uninfected recipient → 12h co-culture between uninfected donor and uninfected recipient → 12h co-culture between infected donor and uninfected recipient → 24h co-culture between uninfected donor and uninfected recipient → 24h co-culture between infected donor and uninfected recipient. NIH ImageJ software was used to analyse blots from 3 biological replicates, performed in triplicates. The expression level of the target gene was normalized to that of β actin (housekeeping gene). Co-culture between differentiated THP-1 macrophages and uninfected cells were taken as a positive control. Differences between infected cells co-culture and control were analysed through student *t* test. * = $p<0.05$ and ** = $p<0.01$

Figure 4.

Effect of *L. aethiopica* (L8G) infected cells on NF-κB signaling during infection spreading. Following infection of differentiated THP-1 macrophages with *L. aethiopica*^{GFP} infected cells, whole cell lysates were collected at 1, 6, 12 and 24 hours after co-culture. Equal amounts (of proteins were resolved by SDS-PAGE and analysed through western blotting. **A.** Densitometry analysis of p-IκB (Ser 32/36) expression. **B.** Densitometry analysis of total IkB expression. **C** Densitometry analysis of total p65 expression. **D.** Densitometry analysis of PKC-δ expression. **E.** Representative blots, left to right lane: 1h co-culture between uninfected donor and uninfected recipient → 1h co-culture between infected donor and uninfected recipient → 6h co-culture between uninfected donor and uninfected recipient → 6h co-culture between infected donor and uninfected recipient → 12h co-culture between uninfected donor and uninfected recipient → 12h co-culture between infected donor and uninfected recipient → 24h co-culture between uninfected donor and uninfected recipient → 24h co-culture between infected donor and uninfected recipient.. NIH ImageJ software was used to analyse blots from 3 biological replicates, performed in triplicates. The expression level of the target gene was normalized to that of β actin (housekeeping gene). Co-culture between differentiated

THP-1 macrophages and uninfected cells were taken as a positive control.Differences between infected cells co-culture and control were analysed through student *t* test. * = $p<0.05$ and ** = $p<0.01$

Figure 5.

L. aethiopica promastigotes transformation into axenic amastigotes in UM54 and JH30 media compared with intracellular amastigotes. **A-C.** Overview *of L. aethiopica* growth in amastigotes-specific media: JH30 and UM54. **A**. Cells concentration in JH30 medium and UM54 medium over 9 days at 32°C. The data represents mean percentage (mean ± SEM) from three independent experiments. **B.** Morphological comparison between *L. aethiopica* transformation in JH30 and UM54. Parasites were stained with Leishmanial stain and observed under 40x magnification. Scale bar=5µm. **C.** Infected human macrophages, stained with Giemsa, containing 15 *L. aethiopica* amastigotes. Scale bar=5µm. **D-G.** SEM of *L. aethiopica* promastigotes transformation into axenic amastigotes in JH30 medium. Stationary phase *L. aethiopica* promastigotes were harvested, washed twice in PBS and re-suspended at a concentration of $1.5x10^6$ cells per ml in a modification of JH30 medium. At specific time points samples were harvested, washed, dehydrated and were critically point dried before being coated in gold for SEM analysis. **D.** Day 0, *L. aethiopica* promastigote showing typical elongated body and flagella. **E.** Day 2, heterogenic population of differently shaped parasites which are likely to represent the various stages of the transformation process. IF1: intermediate form 1, maintained promastigote's elongated shape but appeared wider (the largest part of the body measuring between 3 and 5 µm), shorter (5 and 10 µm) with a flagellum of the same length of the body. IF2: intermediate form 2, showed a rounded/oval body measuring 4 to 6 µm in diameter and 5 to 8 µm in length with flagella measuring at least half the size and, in some cases, just 20% of the promastigotes' flagella. LF, long flagella associated with small rounded bodies were found throughout the transformation process. **F.** Day 6, DF, dividing form, dividing parasites were observed. D. **G.** Day 6, small, rounded paasites resembling amastigotes were identifiable.

Figure 6.

Infection with infected cells model. **A**. Percentage of infected cells following infection with infected cells. Percentage of infected cells was detected via flow cytometry of supernatant containing non-adherent cells (donor) and following EDTA treatment of adherent cells (recipient). All data are mean of 3 biological replicates ± SEM. **B**. Concentration of donor cells was obtained following microscopic counting of trypan blue stained cells at 0h, 1h, 24h, 48h 72h and 96h after infection. Data represent mean concentration of viable cells ± SEM from three independent experiments. Differences between each time point and time 0 were

analysed through one-way ANOVA, Dunnet's multiple comparison test. ** $p<0.005$; ***$p<0.001$, ****$p<0.0001$.

Figure 7.

L. aethiopica trafficking within PMA-treated THP-1 cells. **Ai.** Z-stacked micrographs of GFP-expressing *L. aethiopica* axenic amastigotes's co-localization with an anti-EEA1 primary antibody (subsequently decorated with a Texas red-labelled secondary) 1 hour after infection (arrow). Green: α-GFP; Red: α-EEA1. **Aii.** Percentage of co-localizing of GFP-parasites with EEA1-texa red at all time points tested. Early endosomal co-localization of axenic amastigotes started at 10 min and continued until 4H after infection. No co-localization was detectable at 24H from infection. **Bi.** Z-stacked micrographs of GFP-expressing *L. aethiopica* promastigotes's co-localization with an anti- LAMP-1 specific primary antibody, decorated with an anti-mouse secondary conjugated to Texas red 72 hours following infection (arrow). Green: α-GFP; Red: α-LAMP-1. **Bii.** Percentage of co-localizing of GFP-parasites with LAMP-1-texa red at all time points tested. Late endosomal co-localization of promastigotes was detected at 4H and continued until 72H after infection. **Ci.** Z-stacked micrographs of GFP-expressing *L. aethiopica* axenic amastigote's co-localization with a LAMP-1 specific primary antibody decorated with a Texas red conjugated secondary antibody 4 hour following infection (arrows). Green: α-GFP; Red: α-LAMP-1. **Cii.** Percentage of co-localizing of GFP-parasites with LAMP-1-texa red at all time points tested. Late endosomal co-localization of amastigotes was detected at 1H and continued until 24H after infection. No co-localization was detectable at 10 and 30 min from infection. **Di**. Z- stacked micrographs of GFP-expressing *L. aethiopica's* co-localization with a LAMP-1 specific primary antibody decorated with a Texas red conjugated secondary antibody 4 hour following infection with infected cells (arrow). Green: α-GFP; Red: α-LAMP-1. **Dii.** Percentage of co-localizing of cell-derived GFP-parasites with LAMP-1-texa red at all time points tested. Late endosomal co-localization of amastigotes was detected at 10 min and continued until 24H after infection. PMA treated THP-1 cells were seeded with 12 x 12 x 0.16 mm cover slip and infected with promastigotes, axenic amastigotes and infected cells at Ga 1:10, 1:5, 1:1 ratio. Cell were either fixed with 2% (w/v) PFA and stained with primary antibodies specific for EEA1 or fixed with ice cold methanol and stained with primary antibodies specific for LAMP-1 followed by Texas-Red mouse specific secondary antibodies. Slides were mounted with vectashield H-1200 mounting medium and examined using an LSM880 confocal microscope. Percentage of co-localizing was obtained from ImageJ analysis of a minimum of 3 representative images of infected cells from three independent experiments at various time points after infection. Data are represented individually and as average ± SEM. Scale bar = 5μm.

Figure 8.

Overview of *L. aethiopica* trafficking inside the host macrophages. **A.** Terminally differentiated THP-1 cells were infected with metacyclic promastigotes, newly developed and validated axenic amastigotes and infected cells. **B.** Co-localization with EEA1 was detectable from 30 min to 4 h after infection with axenic amastigotes. **C.** When infected cells were used to start infection, parasites co-localized with LAMP-1 was detectable as early as 10 min after co-culture. **D.** Axenic amastigotes co-localized with LAMP-1 at 1 h after infection. **E.** Late endosomal co-localization with promastigotes was detected from 4 h after infection.

Acknowledgments

We thank Dr Susan Shorter, Thomas Shepherd, Monique Pattrick and Gordon Tang for providing support during immunostaining experiments, Dr Marc Fivaz for critical reading of the manuscript, Samantha Ingram, Rachel Nice, Atiya Raza and Samantha Lewis for technical support. This work was supported by the University of Greenwich VC PhD scholarship.

Author contributions

GG designed the study and supervised all projects. SR and PD supervised the trafficking project and contributed to confocal microscopy experiments and associated data analysis; LH supervised the apoptotic project. MR carried out the trafficking experiment, RR carried out apoptotic pathways' investigation experiments. AD contributed to infection experiments. LP contributed to the apoptotic analysis. GG wrote the manuscripts. All authors discussed the results and implications and commented on the manuscript. All authors read and approved the final version of the manuscript.

Conflict of interest

None to declare.

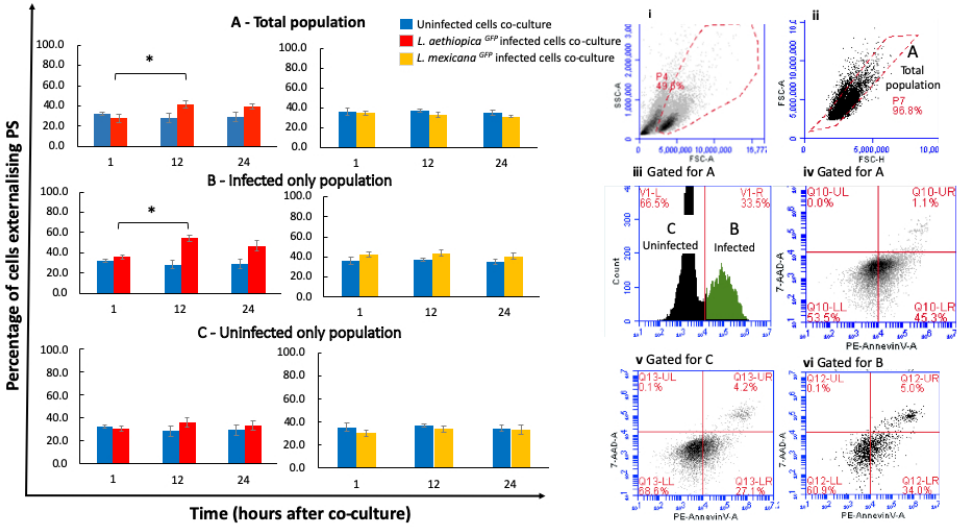

Figure 1.

338x190mm (72 x 72 DPI)

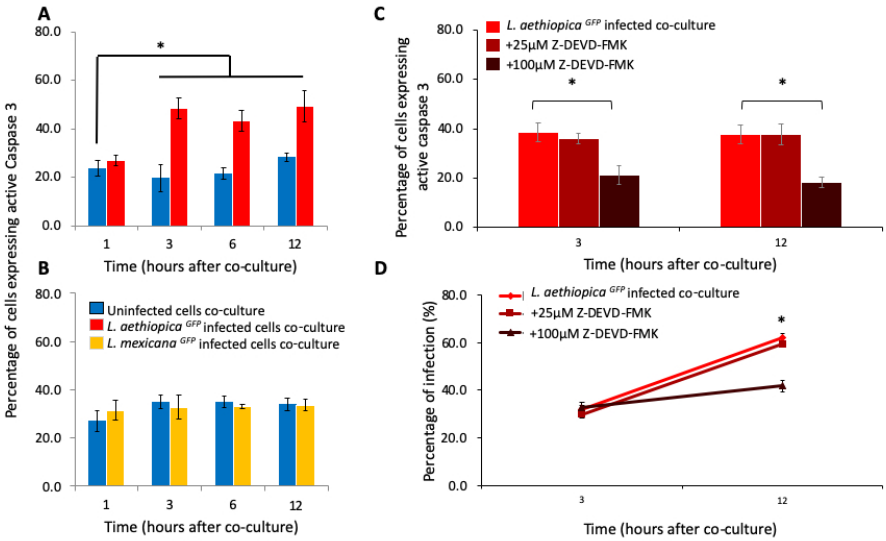

Figure 2.

338x190mm (72 x 72 DPI)

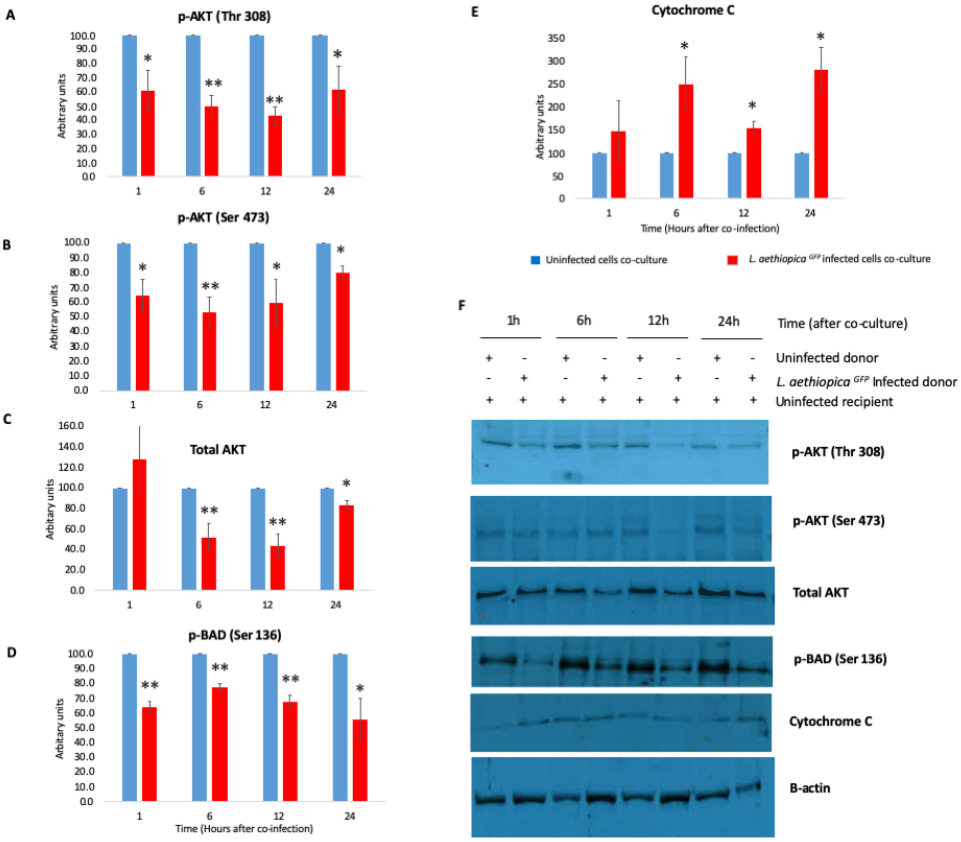

Figure 3.

443x386mm (55 x 55 DPI)

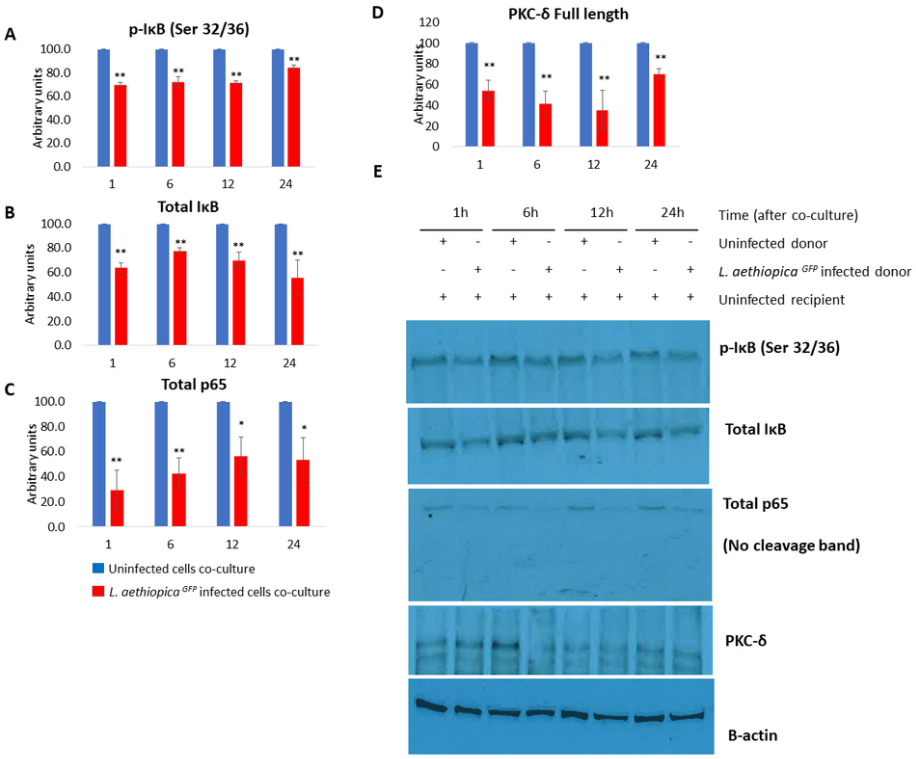

366x299mm (72 x 72 DPI)

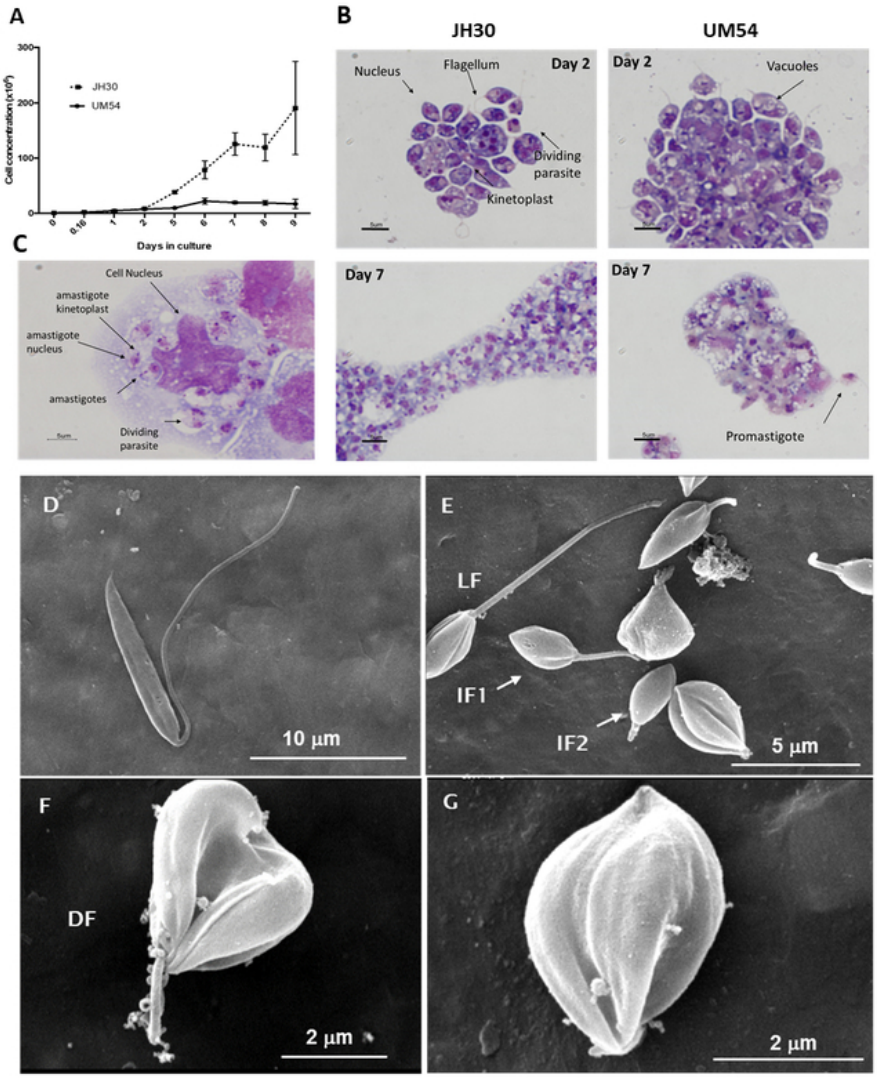

Figure 5. *L. aethiopica* promastigotes transformation into axenic amastigotes in UM54 and JH30 media compared with intracellular amastigotes.

228x306mm (72 x 72 DPI)

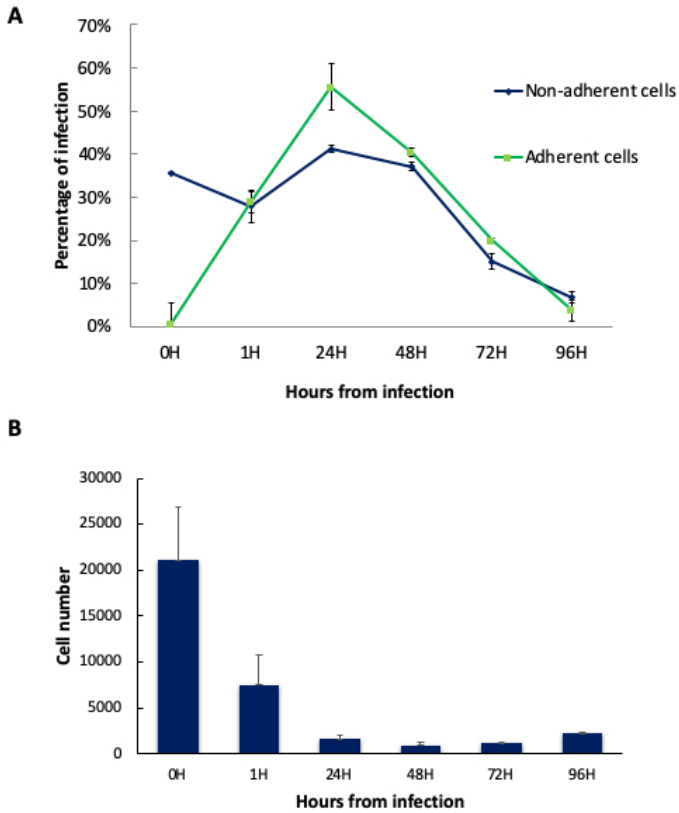

Figure 6. Infection with infected cells model.

190x300mm (72 x 72 DPI)

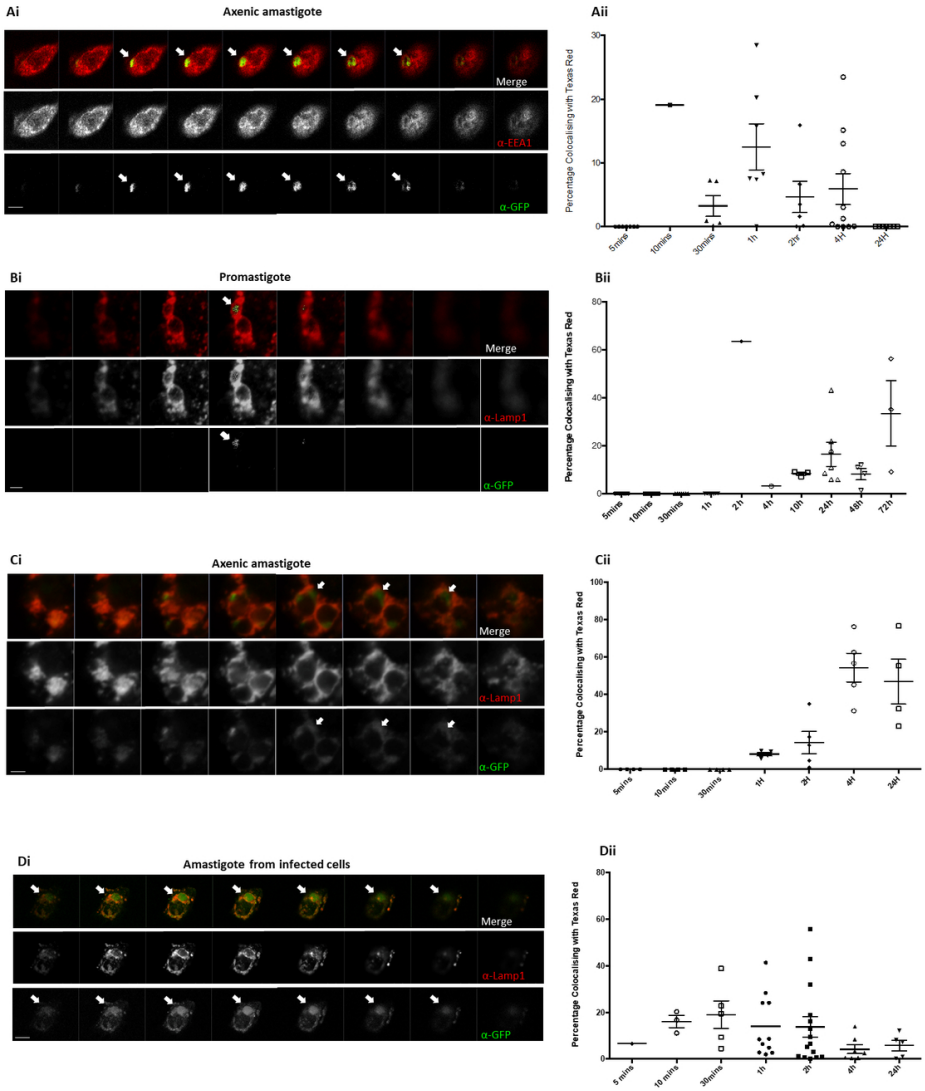

400x510mm (72 x 72 DPI)

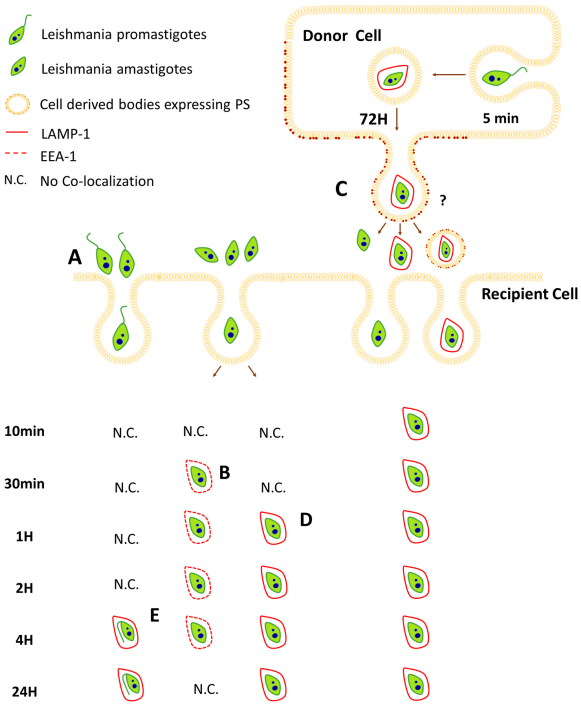

Figure 8. Overview of *L. aethiopica* trafficking inside the host macrophages.

899x699mm (72 x 72 DPI)